Talanta 182 (2018) 193–201

Contents lists available at ScienceDirect

Talanta

journal homepage: www.elsevier.com/locate/talanta

Development and characterization of DNA aptamers against florfenicol: Fabrication of a sensitive fluorescent aptasensor for specific detection of florfenicol in milk

Atefeh Sarafan Sadeghi[a], Mohammad Mohsenzadeh[a,*], Khalil Abnous[b], Seyed Mohammad Taghdisi[c,d], Mohammad Ramezani[b,d,*]

[a] Department of Food Hygiene and Aquaculture, Faculty of Veterinary Medicine, Ferdowsi University of Mashhad, Mashhad, Iran
[b] Pharmaceutical Research Center, Pharmaceutical Technology Institute, Mashhad University of Medical Sciences, Mashhad, Iran
[c] Targeted Drug Delivery Research Center, Pharmaceutical Technology Institute, Mashhad University of Medical Sciences, Mashhad, Iran
[d] Department of Pharmaceutical Biotechnology, School of Pharmacy, Mashhad University of Medical Sciences, Mashhad, Iran

ARTICLE INFO

Keywords:
FluMag-SELEX
Aptamer
Fluorescent assay
Milk analysis
Biosensor
Florfenicol
Graphene oxide

ABSTRACT

Specific ssDNA aptamers for the antibiotic florfenicol (FF) were developed from an enriched nucleotide library using magnetic beads-based SELEX (Systematic Evolution of Ligands by EXponential enrichment) technique with high-binding affinity. After 12 rounds of selection, thirty-six sequences were obtained that were then divided into five major families, according to the primary sequence similarity. Binding affinity analyses of three fluorescently tagged aptamers belonging to different families demonstrated that the dissociation constants (K_d) were in the low nanomolar range (K_d = 52.78–211.4 nmol L^{-1}). Furthermore, to verify the potential application of the aptamers, a fluorescent aptasensor was fabricated for detecting the FF residue in raw milk samples based on the energy transfer between graphene oxide as the acceptor and fluorescently tagged FF-specific aptamer as the donor. Under optimal conditions, the aptasensor displayed a wide linear range from 5 to 1200 nmol L^{-1} and a detection limit of 5.75 nmol L^{-1} with excellent selectivity in milk. The recovery rate in the milk was between 101% ± 0.14% and 110% ± 2.8%, indicating high accuracy. This fluorescent aptasensor possessed considerable potential for rapid analysis of FF in raw milk because of its simplicity of detection. Moreover, the interaction between the aptamer and FF was studied using molecular modeling.

1. Introduction

The indiscriminate use of antibiotics in conventional food-producing animal systems for prophylactic, therapeutic, or growth-promotion purposes may lead to accumulation of their residues in the derived foods [1–3]. This may in turn lead to the development of antibiotic-resistant “superbacteria” [4,5]. Research shows that there have been epidemiologic links between antibiotic use in food-producing animals and the prevalence of antibiotic-resistant infections in humans via the food chain for several decades [6,7]. Therefore, it is crucial to determine the residual antibiotics in animal-derived food products that contain greater than the maximum residue limits (MRL) of antibiotic residues prior to marketing.

Antibiotics of the amphenicol family, including chloramphenicol (CAP), thiamphenicol (TAP), and florfenicol (FF) are effective broad-spectrum antibiotics and exhibit excellent therapeutic indices in veterinary medicine against infections caused by gram-positive and gram-negative bacteria. The antibiotics of the amphenicol family are highly potent inhibitors of prokaryotic protein biosynthesis [8–13]. FF, a fluorinated analogue of TAP, is usually utilized for curative purposes in aquaculture, livestock, and poultry (Fig. S1) [14,15].

The molecular structure of FF is identical to that of CAP and lacks the nitro group on the aromatic ring, a key molecular feature of the dose-unrelated, irreversible aplastic anemia of CAP in humans. However, it is noteworthy that it is theoretically possible for FF to produce serious adverse effects similar to those of CAP. Therefore, FF is not approved for human use although it is used therapeutically for animals [9]. Previously, FF was shown to rapidly metabolize into the dominant metabolite florfenicol amine (FFA) (Fig. S1) in most animals after administration. FFA does not exhibit any antibacterial activity, while it is used as a marker to monitor animal and environmental residues of FF. To ensure the existence of FF residue in edible tissues, the

* Corresponding authors at: Department of Food Hygiene and Aquaculture, Ferdowsi University of Mashhad, Mashhad, Iran. Or Pharmaceutical Research Center, Pharmaceutical Technology Institute, Mashhad University of Medical Sciences, Mashhad, Iran.
E-mail addresses: mohsenza@um.ac.ir (M. Mohsenzadeh), ramezanim@mums.ac.ir (M. Ramezani).

https://doi.org/10.1016/j.talanta.2018.01.083
Received 15 October 2017; Received in revised form 25 January 2018; Accepted 29 January 2018
Available online 01 February 2018
0039-9140/

MRLs have been set at the sum of FF and FFA [16,17] (Table S1).

Currently, the detection of small pharmaceutical molecules has several limitations in terms of lengthy detection time and the requirement of expert personnel and sophisticated equipment, such as high performance liquid chromatography-ultraviolet (HPLC-UV), gas chromatography-mass spectrometry (GC-MS), and enzyme-linked immunosorbent assay (ELISA) [18–20]. Consequently, to overcome the above limitations, it is highly recommended that facile, rapid, sensitive, and cost-effective analytical methods be developed to enable the accurate detection of FF and FFA residues [21,22].

Graphene-based nanomaterials have been broadly used for developing sensing platforms because of their unique features, such as high planer surface and remarkable electrical as well as mechanical properties [23,24]. Graphene oxide (GO) is a two-dimensional (2D) graphitic carbon material capable of adsorbing single-stranded DNA (ssDNA) by hydrophobic and π-π stacking interactions between the nucleotide bases and GO [24–29]. GO has been used as an excellent energy acceptor in energy transfer-based fluorescence sensors, with the ability to quench fluorescent probes as an electron donor. Hence, GO possesses substantial potential for the preparation of the extremely sensitive fluorescence-based sensors platform meant for bio-molecular recognition [26,30,31].

Aptamers are synthetic short ssDNA, or RNA nucleic acid molecules, obtained through randomized sequence pools using an in vitro screening procedure called SELEX (Systematic Evolution of Ligands by EXponential enrichment) [32,33]. The diversity of the structures displayed by a random DNA fragment library permits the selection of tight binding aptamers toward given targets, ranging from small organic molecules to cells [34–38]. Aptamers offer advantages over antibodies, including high stability and specificity, target adaptability, chemical synthesis with high purity, reproducibility, easy modification, simple storage, cost-effectiveness, low immunogenicity, and resistance to denaturation and degradation [39,40]. Therefore, the use of aptamers is gaining popularity in various fields, including drug delivery and bioanalysis [22].

In the current study, we developed novel ssDNA aptamers against FF and FFA with high affinity, using the FluMag-SELEX technique with magnetic beads [34]. Thereafter, the capable aptamers with high affinity were selected to fabricate a fluorescence-based aptasensor using GO. In the final stage, the fluorescence-based aptasensor was used for simple and highly sensitive and selective detection of FF residue in milk.

2. Materials and methods

2.1. Chemicals and reagents

FFA, FF, CAP, enrofloxacin, amoxicillin, tetracycline and GO were purchased from Sigma-Aldrich (www.sigmaaldrich.com). Tosyl-activated magnetic bead (Dynabeads M-280 Tosyl-activated) was obtained from Invitrogen (www.fishersci.com). The ssDNA library comprising a central sequence with 43 random nucleotides (5´-GCTGTGTGACTCCT GCAA-N43-GCAGCTGTATCTTGTCTCC-3´) and both forward (5´-GCT GTGTGACTCCTGCAA-3´) and 5´phosphorylated reverse (5´-phosphate-GGAGACAAGATACAGCTGC-3´) primers were synthesized by Bioneer (http://www.bioneer.com/,South-Korea) [41]. The reverse primer was 5´phosphorylated to allow the digestion of the antisense strands by lambda exonuclease [42]. ATTO647N-labeled oligonucleotides were synthesized by Microsynth (http://www.microsynth.ch/,Swiss). Reagents for polymerase chain reaction (PCR), including the PCR buffer, $MgCl_2$, dNTP and *Taq* DNA polymerase were supplied by SinaClon (http://www.sinaclon.com/Iran). Ultrapure agarose was ordered from Invitrogen. All other chemicals, including NaCl, KCl and Tris were purchased from Merck (http://www.merck.com).

2.2. Immobilization of FFA on magnetic beads

For the immobilization process, we used FFA for covalent immobilization to tosyl-activated magnetic beads surface. Covalent attachment of the amino group of FFA was performed in borate buffer (0.1 mol L^{-1}, pH 9.5) by overnight incubation of FFA (10 mmol L^{-1}) for reaction with beads under gentle rotation and tilting at 37 °C. The binding rate for 30 mg Dynabeads M-280 tosyl-activated (1 mL) is about 3–6 μmol of the target. Thereafter, for blocking the unreacted *p*-toluenesulfonyl (tosyl) groups of the beads, they were incubated with ethanolamine (1 mol L^{-1}, pH 8.0) for 6 h at 37 °C with mild shaking. After a few washes, the beads were re-suspended in the phosphate-buffered saline (PBS) buffer, and stored at 4 °C until use. An additional aliquot of ethanolamine-coated magnetic beads was prepared under the same conditions as those used in the counter selection steps.

The FFA coupling was confirmed using infrared (IR) spectroscopy (FTIR spectrometer, Perkinelmer, USA) by acquiring the spectra of the FFA, FFA-coated beads, and ethanolamine-coated beads. The IR spectra were recorded at room temperature in the range 400–4000 cm^{-1} with a resolution of 4 cm^{-1}, and each spectrum was the average of 100 scans.

2.3. In vitro selection of aptamers (SELEX)

In vitro selection was performed to separate specific aptamers for FF. Before each round of SELEX, a homogeneous suspension of 3 mg FFA-coated magnetic beads (FMBs) was washed several times with the binding buffer (BB) (100 mmol L^{-1} NaCl, 5 mmol L^{-1} KCl, 2 mmol L^{-1} $MgCl_2$, 1 mmol L^{-1} $CaCl_2$, 20 mmol L^{-1} Tris–HCl [pH 6], and 0.02% Tween 20 [pH 7.6]) and finally diluted in 100 μL BB.

In the first SELEX round, 2 nmol random ssDNA library (containing approximately 10^{15} molecules) as the initial pool was dissolved in the BB. For refolding the library, it was incubated for 10 min at 90 °C followed by quick cooling to 4 °C; thereafter, it was kept at this temperature for 15 min. Finally, it was placed at room temperature (RT) for 7 min. Then, 3 mg washed FMBs (30 mg beads mL^{-1}) were added to the renatured library and incubated at RT for 45 min with tilting and rotation. The unbound ssDNA molecules were removed by washing several times with BB. The bound sequences were eluted from the ssDNA/FMBs complex by dissolving them in 100 μL elution buffer (EB) (3.5 mol L^{-1} urea, 10 mmol L^{-1} EDTA, 40 mmol L^{-1} Tris-HCl [pH 8.0], and 0.02% Tween 20 [pH 8.0]) for 10 min at 80 °C with mild shaking, followed by the magnetic separation of the FMBs, leading to the recovery of the ssDNA molecules. The aforementioned procedure was repeated 4 times to elute all traces of the bound ssDNA. The collected ssDNA pool was further purified and concentrated through ethanol-precipitation at −80 °C for 30 min. The eluted ssDNAs were re-suspended in 30 μL distilled water and amplified with PCR. The amplification was performed as follows: an initial activation through pre-denaturation at 94 °C for 5 min followed by denaturation cycles at 94 °C for 30 s, annealing at 60 °C for 30 s, elongation at 72 °C for 30 s, and finally an additional elongation step at 72 °C for 3 min. The PCR products were controlled by agarose gel electrophoresis in terms of selection of the optimum PCR cycle without primer-dimer formation and non-specific products. Purification of the PCR products was carried out using a NucleoSpin® Extract II kit (Macherey-Nagel, Germany, www.mn-net.com) according to the manufacturer's protocol. For the next round of enrichment, all purified dsDNAs were digested to ssDNAs using lambda exonuclease (#EN0562) (Thermo Scientific, Schwartz, Germany, https://www.thermofisher.com) that selectively digests the 5´-phosphorylated antisense sequences of dsDNA without altering the sense strand. The concentration of the obtained ssDNA fraction was measured using NanoDrop spectrophotometer (NanoDrop UV–Vis spectrophotometer, USA) and used in the next selection round as the starting pool. To increase the specificity of the selected ssDNA molecules and eliminate the undesired ssDNAs, counter selections with

ethanolamine-coated beads were performed from the third round of the SELEX process.

In our study, 12 rounds of SELEX were performed. To obtain aptamers with high affinities and specificities, the selection strength was improved by gradually increasing the number of washes from 5 to 12 and the amount of ethanolamine-coated beads in counter steps and finally, by reducing the incubation time from 45 min to 30 min.

2.4. Monitoring of the enrichment of aptamer pool

After 12 selection rounds, some rounds were chosen for the enrichment analysis. The oligonucleotides of each round were amplified using ATTO647N-labeled forward primer and 5′-phosphorylated reverse primer. Then, each of ATTO647N-labeled ssDNA of the initial library, 3th, 7th, 8th,10th,11th and 12th rounds of SELEX (3000 ng) in 100 µL Tween–free BB were mixed and incubated with the washed FMBs at 37 °C for 30 min with mild shaking. Thereafter, the beads were washed five times with BB. The bound sequences were eluted twice by the incubation of the ssDNA/FMBs complex with EB for 10 min at 80 °C under mild shaking. The fluorescence measurements of the eluted ATTO647N labeled-sequences were conducted using a fluorimeter to select the best round. The florescence intensity of each sample was determined at 665 nm in 96-well plates using a Synergy H4 microplate reader (BioTeK, USA). The ATTO647N-labeled ssDNA library was used as a negative control.

2.5. Cloning, sequencing, and alignment of sequences

The ssDNA pool from the eleventh SELEX round was amplified with unlabeled primers and cloned into *Escherichia coli* Top10 using InsTAclone PCR Cloning kit (Life Technologies, EU, https://www.thermofisher.com) according to the manufacturer's protocol. Following overnight incubation, the white colonies from the culture plate containing X-Gal/IPTG and ampicillin were cultured separately. Subsequently, colony-PCR was performed to confirm if the sequence was inserted. Thereafter, the plasmids were purified using Denazist Plasmid DNA isolation kit (Denazist Asia, Iran, http://www.denazist.com) and sequenced (Bioneer, South-Korea, http://www.bioneer.com/, South-Korea). To categorize and align the obtained sequences, their phylogenic tree was drawn using the DNAMAN software. The internet tool Mfold was also used to predict the secondary structure models of the sequences by the free-energy minimization algorithm [43].

2.6. Determination of the dissociation constants (K_d) of individual aptamers

Four modified ssDNA aptamer candidates, labeled with ATTO647N, were synthesized by Microsynth (http://www.microsynth.ch/, Swiss). To measure the binding affinities of the aptamer candidates against FF, labeled-sequences were examined using a method similar to the SELEX process. For the binding analyses, a constant number of FMBs (0.3 mg) was washed and suspended in 100 µg/mL salmon sperm DNA solution and BB at 37 °C for 2 h on a rotary shaker; thereafter, it was washed with BB. Nine concentrations, ranging from 0 to 1000 nmol L^{-1} of each ATTO647N-labeled aptamer, were denatured and renatured in 100 µL Tween-free BB as described previously for thermal equilibration. These prepared solutions were incubated with FMBs for 30 min at RT with mild shaking.

The unbound aptamers were separated by washing several times. The bead-bound aptamers were eluted twice by incubation of the aptamer/FMBs complex with 100 µL EB at 80 °C for 10 min with shaking. The fluorescence intensity of the eluted ssDNA was measured. The ATTO647N-labeled ssDNA library was employed as a negative control.

The dissociation constant (K_d) value was calculated using the dependence of the fluorescence intensity of specific binding (Y) on the concentration of aptamer (X) according to the equation $Y=B_{max} \times X/(K_d + X)$ and the non-linear regression analysis using the GraphPad Prism software. Data are presented as mean ± standard deviation (SD) values, n = 3.

2.7. Molecular modeling studies

To investigate the association mechanism between the developed aptamer (Apt 125) and FF, the three-dimensional structures of both molecules were drawn using appropriate series of software, including Mfold, RNA Composer, Chimera 1.8.1, ViewerLite 4.2, and ChemBioOffice Ultra 8.0. The chemical structures of both molecules were minimized in terms of energy with the HyperChem 7.0 program using the AM1 semi-empirical technique.

Before running AutoDockTools 1.5.4, all hydrogen atoms and Gasteiger charges were added to the oligonucleotide molecule in the rigid form. The grid box was applied to all loops. The Lamarckian genetic algorithm was chosen to prepare the docking-parameter file with 200 replications. We used the default settings, and their interactions were examined using the docking program. The computation results of docking were reordered based on the binding energy. The interactions and conformations of the aptamer-ligand were assessed using Swiss PDB viewer 3.7 and ViewerLite.

2.8. Performance of the selected aptamers in FF detection in phosphate buffer saline (PBS) and milk

In order to approve the capability of the selected aptamers (Apt122 and Apt125) for the detection of FF, a fluorescence-based aptasensor was developed using GO. In this aptasensor, 50 µL working solution containing 70 nmol L^{-1} ATTO647N-aptamer solution in 20 mmol L^{-1} PBS was mixed with 50 µL GO solution (25 µg/mL). This solution was incubated for 30 min at RT. For FF sensitivity measurement, appropriate concentrations of FF and FFA solution (0–7000 nmol L^{-1}) were mixed with the resulting solution to obtain a final volume of 150 µL. Finally, the fluorescence intensity of the incubated solution was monitored at 665 nm. The selectivity of the sensor was investigated in the presence of 3000 nmol L^{-1} enrofloxacin, CAP, amoxicillin, tetracycline, FFA and FF.

To evaluate the applicability and reliability of the developed aptasensor for FF detection in the real sample, it was used to determine and assess the recovery of the residual amount of FF in milk (diluted 10-fold with the PBS buffer). Milk samples were contaminated with different concentrations of FF (5, 150, 1200 nmol L^{-1}) on different days and subjected to bioanalysis using the prepared aptasensor. Milk sample without FF was used as negative control.

3. Results and discussion

A ban has been imposed on the use of CAP in food-producing animals; therefore, FF with similar antibacterial activity is increasingly used. Moreover, FF exhibits antibacterial activity against some CAP-resistant bacterial strains. Although FF is safer than CAP, its presence in the final animal products exhibits potential hazards for humans who consume it. There are various traditional methods for detecting FF; however, most of them are unsuitable for high capacity screening, are expensive, exhaustive, and require sophisticated facilities and expert personnel. Aptamer-based biosensors offer newer options to overcome these limitations.

3.1. Immobilization and characterization of target on the magnetic beads

In order to separate the small target molecules during the SELEX process, they were firmly immobilized onto solid support matrixes. Magnetic bead matrixes have appropriate surface properties for the isolation of target-bound sequences from those with no affinity for the target, using a magnetic stand (33, 37).

In our study, tosyl-activated magnetic beads were used for the in

vitro selection of aptamer candidates from the nucleic acid pool. FFA has one amine (NH_2) functional group; therefore, tosyl-activated bead was selected for target molecule immobilization. Tosyl is a leaving group that can be substituted by primary amine groups (Fig. S2). Excess FF was used to ensure that all the binding sites of the magnetic beads were occupied by FF. The unreacted tosyl groups on the beads surface were finally blocked with ethanolamine. The formation of the amide-linkage was confirmed using IR spectroscopy.

As shown in the FT-IR spectrum (Fig. S3A), a substitution reaction of ethanolamine on the surface of tosyl-activated Dynabeads M-280 was verified by the disappearance of a distinct peak corresponding to C=C aromatic vibration around 1709 cm^{-1}, one of the characteristic features of tosyl-activated beads.

Fig. S3B is the FT-IR spectrum of FFA, wherein the strong peak at 1000 cm^{-1} represents C-F vibration. In addition, the peaks at 1153 cm^{-1} and 1311 cm^{-1} were assigned to symmetric and asymmetric stretch vibrations of sulfones. Moreover, two peaks at 3300–3400 cm^{-1} are related to the N-H stretching vibration of the primary amine.

FFA conjugation onto the surface of tosyl-activated beads was confirmed by FT-IR spectrum (Fig. S3C). The existence of a peak around 1000 cm^{-1} corresponding to C-F stretching suggests the presence of FFA in the conjugate structure. Moreover, the disappearance of the primary amine peaks around 3300–3400 cm^{-1} in the target-coated beads and the appearance of peak corresponding to secondary amine confirmed the successful coupling of FFA via the amine group. The broad peak appeared between 2500 cm^{-1} and 3300 cm^{-1} due to the presence of the ethanolamine on the bead surfaces.

3.2. Aptamer enrichment through the SELEX rounds

The selection of aptamers that specifically bind FF was accomplished by the random ssDNA library using the Flu-Mag SELEX process. During each round, the non-specific bound ssDNA molecules were removed through excessive washing. The ssDNAs bound to FF were amplified with PCR. The PCR products were then purified and digested to ssDNAs, implementing lambda exonuclease. Nine counter selection steps were performed using ethanolamine-coated beads to avoid non-specific aptamers (Fig. 1). After twelve rounds of selection, the binding affinities of the library, 3rd, 7th, 8th, 10th, 11th and 12th rounds were monitored using fluorescence spectroscopy. The obtained results demonstrated that the eleventh round displayed the highest fluorescence among all other rounds (Fig. S4). By contrast, the fluorescence intensity of the library and the eleventh round were measured for counter beads using fluorescence spectroscopy. Fig. S5 demonstrates that the 11th round exhibited significantly lower affinity to counter beads compared to the affinity of the library to the counter beads. This could be attributed to the presence of up to 10^{15} random DNA fragments in the library; however, in the 11th round, the random DNA fragments were much lower because of the SELEX procedure. Thus, the ssDNA pool from the 11th round was cloned and sequenced.

3.3. Cloning and clustering

Forty potential white or light blue clones that carried the aptamer fragments were selected and sequenced. The obtained data resulted in the identification of thirty-six novel sequences. The sequences were evaluated using the DNAMAN software based on their homology and phylogenetic tree. All the isolated aptamers were classified into five families (Fig. S6), and four aptamers were selected and their affinities to FF analyzed (data not shown). Finally, aptamers 1, 85, 122, and 125 were selected for developing the biosensing platform against FF/FFA.

3.4. Characterization of the selected aptamers

To evaluate the affinities of the four aptamer candidates against their target, their dissociation constants (K_d values) were determined using fluorescence-based affinity assays. Binding reaction was conducted using a constant number of FMBs as the target and different concentrations of each ATTO647N-labeled aptamer (0–1000 nmol L^{-1}). After excessive harsh washing, aptamers were eluted, and the specific binding affinities were determined.

Fig. S7 illustrates the non-linear regression of the binding affinity of the four selected aptamers to the target. In this regard, the K_d values of all aptamers (Apt1, Apt85, Apt122, and Apt125) were calculated as 52.78 nmol L^{-1}, 96.51 nmol L^{-1}, 211.4 nmol L^{-1}, and 759.7 nmol L^{-1}, respectively. The obtained results indicated higher K_d values for Apt1 and Apt85, confirming the weak binding affinity of these aptamers to target molecules and their inappropriateness for further study. The differences in the binding modes of these four aptamers could be attributed to the impact of ionic interactions along with their particular motifs and three dimensional folding properties [44]. The sequences and K_d values of the selected aptamers have been shown in Table 1.

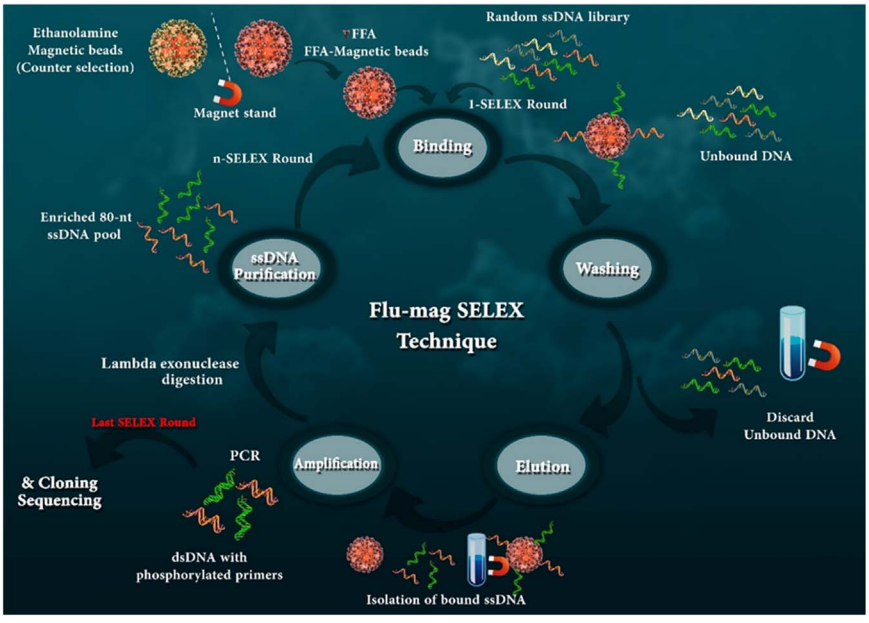

Fig. 1. The selection procedure of FF specific aptamers by SELEX using magnetic beads.

Table 1
The sequences and K_d values of four selected aptamers against FF and FFA by SELEX.

Name	Length	Sequences 5′→ 3′	K_d (nmol L^{-1})
Apt1	80	GCTGTGTGACTCCTGCAACGTTCGTTACCTTGATTAGTCCGTGCAGTGCATATAACGCGGTGCAGCTGTATCTTGTCTCC	759.7
Apt85	80	GCTGTGTGACTCCTGCAAGACCCATTTGTATGACAGTTTTACCGCGCCGTGAATTATCGTTGCAGCTGTATCTTGTCTCC	211.4
Apt122	81	GCTGTGTGACTCCTGCAAGCCGGGAACATGCCGCGTGCATAAGCAGCCCCTTCACCCTGCAGCAGCTGTATCTTGTCTCC	96.51
Apt125	80	GCTGTGTGACTCCTGCAAGGTCCATTCAAGTCGTAGGTTTGCCTTCAGCCTCAACGCTTACGCAGCTGTATCTTGTCTCC	52.78

3.5. Analytical application of Apt122 and Apt125 for FF and FFA detection

3.5.1. Design strategy

Compared to Apt1 and Apt85, Apt122 and Apt125 showed better binding affinities. Consequently, Apt122 and Apt125 were selected for developing the biosensing platform. An ideal platform for biosensing is cost effective, simple, and fast [45]. GO provides an inexpensive platform for fluorescence-based biosensors; therefore, we used GO as an energy acceptor (quencher) in the developed aptasensors and ATTO fluorescence dye as an energy donor.

In the absence of a target molecule, ATTO-tagged aptamer was adsorbed onto the GO surface via л-л stacking interactions between the aromatic nucleobases of ssDNA and the sp^2-hybridized carbons of GO. The fluorescence of ATTO647N-labeled aptamer was quenched because of the energy transfer from the ATTO fluorescence dye to the GO sheets [46,47].

In the assay process, the ATTO-tagged aptamer is released from the GO by the specific interaction between the aptamer and the target molecule. Consequently, fluorescence intensity increased (Fig. 2). The fluorescence recovery may be explained by the relatively weaker л-л stacking interaction between the FF/aptamer complex and the GO sheet. It was demonstrated that the prepared GO-based aptasensor was highly sensitive to FF and FFA detection in both buffer and milk.

3.5.2. Optimization of assay conditions

In this study, the optimum GO concentration was obtained to achieve highest ATTO647N-labeled aptamer quenching activity. Fig. S8 shows the fluorescence quenching of the aptamer at different GO concentrations. The fluorescence intensity decreased substantially when GO was added into the aptamer solution. We found that the 25 μg/mL GO quenched about 90% of the fluorescence intensity of the ATTO647N-labeled aptamer, while the addition of higher concentrations of GO did not exhibit further quenching activity. Thus, this fixed concentration of GO (25 μg/mL) was used for preparing the aptasensor.

To confirm the coupling of the aptamer to GO, 2.5% agarose gel electrophoresis was implemented (Fig. S9). The gel electrophoresis results demonstrated the formation of the aptamer/GO complex. Agarose gel electrophoresis is a molecular weight-dependent technique; the aptamer appeared at nearly 100 bp with a bright and obvious band (lane 3). When the aptamer/GO complex was added, no movement of the aptamer was observed (lane 4), suggesting that the aptamer was totally captured by GO and unable to enter the gel.

To further investigate the processes of turn-on/off fluorescence by the ATTO647N-labeled aptamer/GO complex, we examined the influence of the incubation time of ATTO-647N-labeled with GO suspension (Fig. S10). The maximum fluorescence quenching activity was obtained after 30 min of incubation. The obtained result verified that the fluorescence-quenching process of labeled aptamer was conducted in a time-dependent manner.

3.5.3. Target detection

Fig. 3A represents the relative fluorescence changes of the labeled Apt125/GO complex in the presence of different FF concentrations. The relative fluorescence intensity increased after the addition of the target molecule (FF) into the labeled Apt125/GO complex.

In this respect, a linear range was obtained from 5 to 5000 nmol L^{-1}. In addition, the detection limit of the developed aptasensor was estimated as 1.58 nmol L^{-1} for FF in the PBS medium, based on three folds standard deviation of the blank signal (3σ)/Slope.

The relative fluorescence intensity of the labeled-Apt122/GO complex in the presence of different concentrations of FFA is shown in Fig. 3C.

The relative fluorescence intensity of the sensor substantially increased with the increasing concentration of the target from 5 to 7000 nmol L^{-1}. The calibration curve for FFA detection has been shown in Fig. 3D, and the linear range was obtained from 5 to 1200 nmol L^{-1}

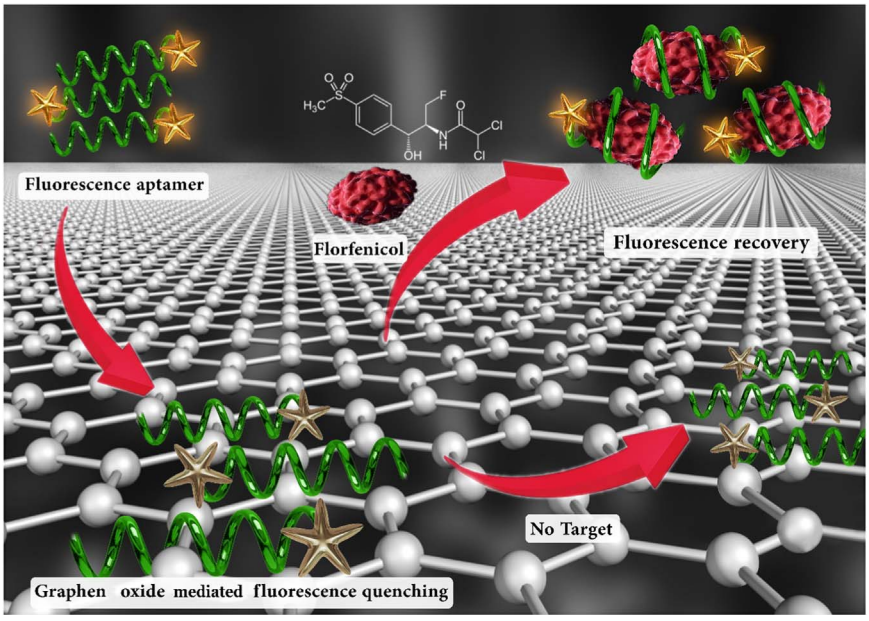

Fig. 2. Schematic illustration of the biosensing strategy involved in the turn-on fluorescent aptasensor based on the GO for FF detection.

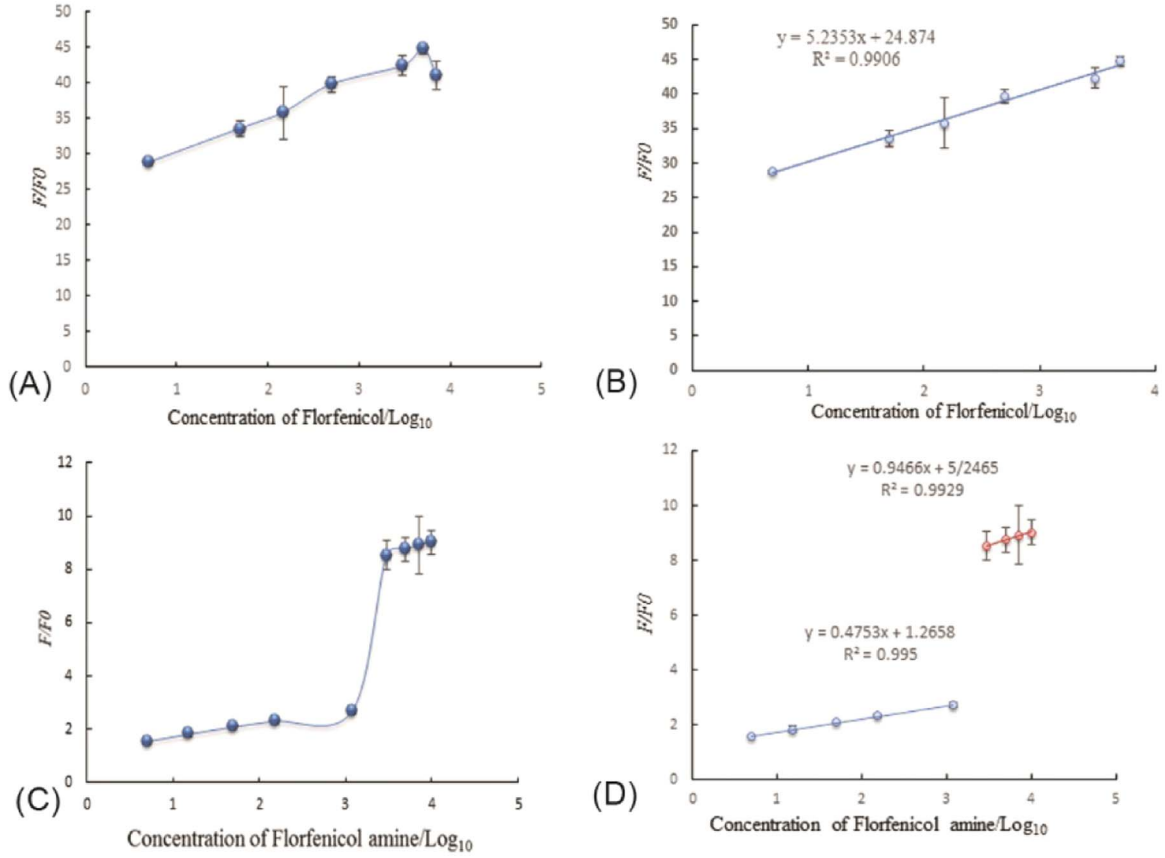

Fig. 3. (A) Relative fluorescence intensity of labeled Apt125/GO complex after incubation with different concentrations of FF (5–7000 nmol L^{-1}). (B) Calibration curve of the developed aptasensor in PBS for FF detection with Apt 125. (C) Relative fluorescence intensity of labeled Apt122/GO complex after incubation with different concentrations of FFA (5–7000 nmol L^{-1}). (D) Calibration curve of the designed aptasensor in PBS for FFA detection with Apt 122. F_0 and F are the fluorescence intensities of ATTO647N at 665 nm in the absence and presence of target, respectively (n = 3).

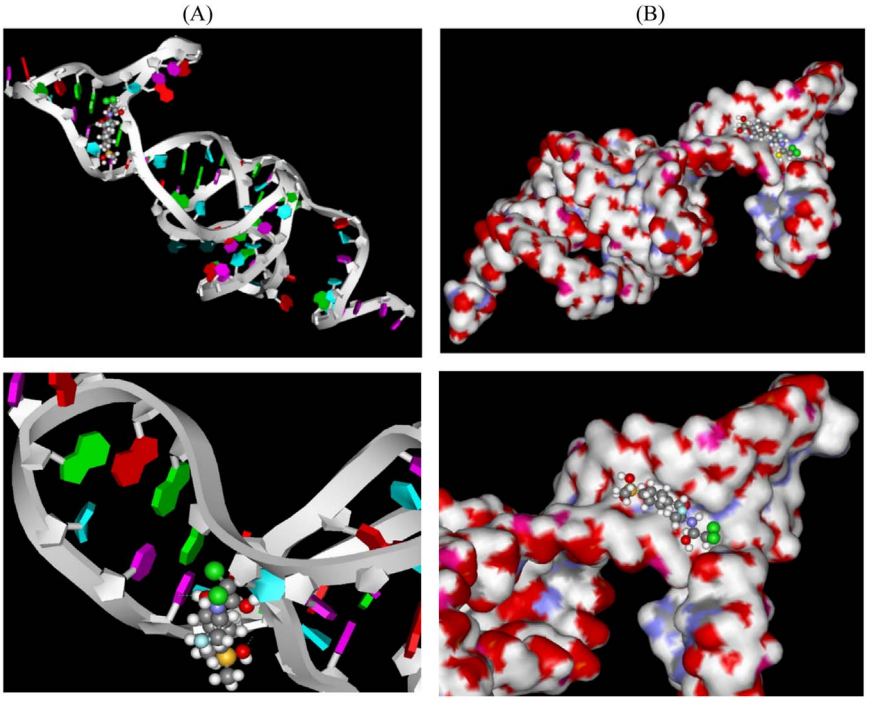

Fig. 4. Molecular docking results depicting interaction between aptamer 125 and florfenicol. (A) Ring display and (B) surface added display.

and 3000–7000 nmol L^{-1}. Some aptasensors have been reported to have two linear ranges owing to the nature and intrinsic properties of their aptamers [48,49]. For this aptasensor, the detection limit was estimated at 2.09 nmol L^{-1}.

Table S2 presents the analytical performances of various techniques for the determination of FF and FFA [20,50–58]. In addition, Table S3

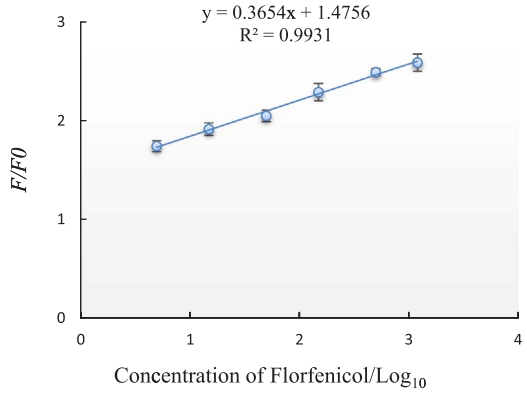

Fig. 5. Standard curve for the determination of FF using the developed aptasensor upon addition of different concentrations of FF in milk.

indicates the fluorescence aptasensors developed for detecting amphenicol [59–67]. To our knowledge, thus far, no report on the preparation of aptasensors for FF detection has been published. It is noteworthy that the previously reported CAP-aptasensor was unable to detect FF; thus, there is a need to develop an inexpensive and rapid aptasensor for FF detection [60,68,69]. Compared to the other reported detection techniques, this newly constructed aptasensor is cheaper, simpler, and has more acceptable sensitivity. Furthermore, this sensor exhibited low limit of detection (LOD) and good feasibility for FF detection in a real milk sample.

3.6. Selectivity of graphene fluorescence aptasensor

To evaluate the selectivity of the prepared aptasensor, fluorescence responses of the fabricated aptasensor towards FF and FFA versus that toward other antibiotics, such as enrofloxacin, amoxicillin, tetracycline, and CAP were measured under similar experimental conditions. As shown in Fig. S11, the addition of 3000 nmol L^{-1} of either FF or FFA significantly increased the fluorescence intensity of the sensor, while no obvious fluorescence restoration was observed for other antibiotics.

The results clearly demonstrated that the developed aptasensor was capable of detecting both FF and FFA with high specificity while having no cross-reaction with other molecules, even those with similar structures. This ideal selectivity is attributed to the intrinsic properties and the unique 3D-foldings of the selected aptamers (Apt 122 and Apt125), leading to specific target-recognition [70,71].

3.7. Assessment of the Apt125-FF binding properties by molecular modeling

The conformational and modeling information is a valuable guideline for better comprehension of the interaction between aptamers and their targets. In the present study, we found that between 200 replications, the target was located inside the loop (T11-A29) 79 times. Therefore, the region with the best result was selected for further analysis. In contrast, it appeared that two hydrogen atoms of FF would bind the loop nucleotides of aptamer (T11-A29), including C12 and G30 (Fig. 4). As shown in Fig. 4, the small loop between T14-A18 was merged with other loops (T11-A29), probably because of steric inhibition. Therefore, this region is the potential area for truncation.

However, the results of computations may be misleading; therefore, the real dissociation constant should be determined experimentally. In addition, the aptamer was considered in a rigid form; however, it is obvious that such molecules are flexible and dynamic. For example, the result of the computational study showed that the K_d value of Apt125 was 18.14 μmol L^{-1}, while the experimental results demonstrated that the K_d of the aptamer was 52.78 nmol L^{-1}. However, this may provide information enabling better employment of the novel features of aptamer-target complexes.

3.8. FF detection in milk sample

In order to investigate the feasibility of the prepared aptasensor, milk sample was selected as a real sample for detecting the residual quantity of FF. Thus, milk was spiked with a series of known concentrations of FF. Fig. 5 illustrates the interactions between GO and ATTO647N-labeled Apt 125 in the presence of different FF concentrations in milk samples. The obtained results demonstrated the potential applicability of the prepared aptasensor for detecting FF in real samples. The calculated LOD and limit of quantitation (LOQ) were 5.75 nmol L^{-1} (2 μg kg^{-1}) and 18.9 nmol L^{-1}, respectively, indicating that this aptasensor can be implemented to detect very low levels of FF in milk Scheme 1.

The applied detection strategy exhibited a good linear response from 5 to 1200 nmol L^{-1} of FF. To investigate the validity and reliability, three fluorescent aptasensors were prepared in different days (each experiment was repeated thrice). The detection accuracy of the

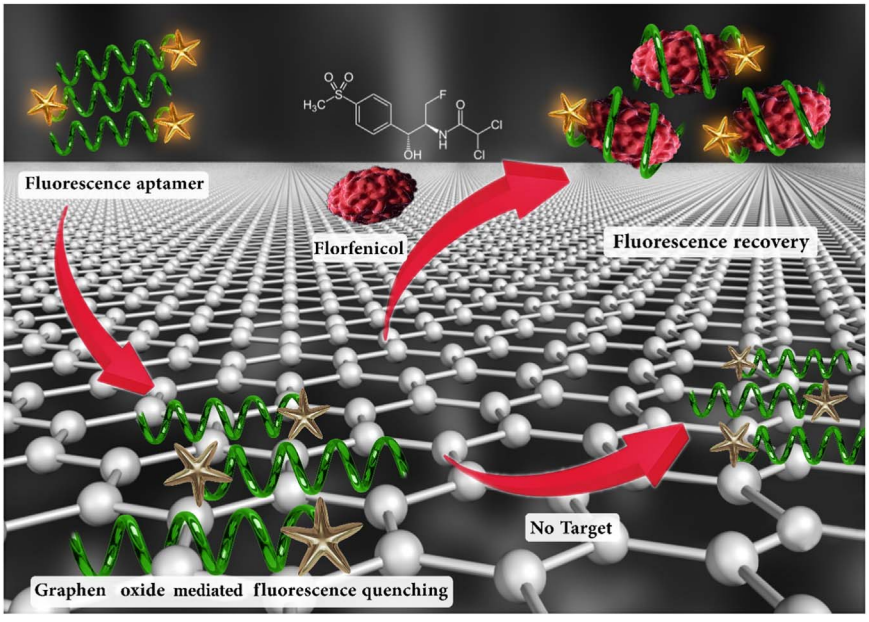

Scheme 1. Schematic illustration of the biosensing strategy involved in the turn-on fluorescent aptasensor based on the GO for FF detection.

Table 2
Recovery of FF concentrations in milk using the developed fluorescence-based aptasensor.

FF spiked (nmol L^{-1}, n = 3)	Found (nmol L^{-1})	Recovery (100% ± SD, n = 3)
15	16.6	110% ± 2.8
150	152.5	101% ± 0.14
1200	1226.7	102% ± 0.07

prepared aptasensor was assessed, and the obtained data indicated that the recovered relative fluorescence was between 101% and 110%. Therefore, we could conclude that this sensing platform demonstrated the ideal reliability for FF detection in a real sample. Based on the results of the recovery assay, the method was reproducible because the relative standard deviations (RDSs) were below 2.8% (Table 2).

4. Conclusions

In this study, we successfully developed aptamers that have the ability to specifically and selectively recognize and quantify FF and FFA. By using a dye-labeled aptamer and GO-based platform, FF and its major metabolite (FFA) were detected in milk samples. The developed GO-based fluorescence aptasensor has several unique features, including high selectivity, high sensitivity, and simplicity of target detection. This aptasensor exhibited a high capability of detecting FF and FFA in a short period of time (90 min) under the established MRL values (LOD = 5.75 nmol L^{-1}), superior to that in other reported techniques.

Acknowledgment

Financial support for this study was provided by the Mashhad University of Medical Sciences and the Ferdowsi University of Mashhad (grant number 3/28252). This report has been extracted from the Ph.D. thesis of Atefeh Sarafan Sadeghi.

Conflict of interest

The authors report no conflicts of interest regarding this article.

Appendix A. Supporting information

Supplementary data associated with this article can be found in the online version at http://dx.doi.org/10.1016/j.talanta.2018.01.083.

References

[1] J.F. Prescott, Antimicrobial use in food and companion animals, Anim. Health Res. Rev. 9 (2008) 127–133.
[2] S.A. McEwen, P.J. Fedorka-Cray, Antimicrobial use and resistance in animals, Clin. Infect. Dis. 34 (2002) S93–S106.
[3] N. Sanvicens, I. Mannelli, J.P. Salvador, E. Valera, M.P. Marco, Biosensors for pharmaceuticals based on novel technology, Trends Anal. Chem. 30 (2011) 541–553.
[4] K. Bush, P. Courvalin, G. Dantas, J. Davies, B. Eisenstein, P. Huovinen, G.A. Jacoby, R. Kishony, B.N. Kreiswirth, E. Kutter, Tackling antibiotic resistance, Nat. Rev. Microbiol. 9 (2011) 894–896.
[5] E.D. Brown, G.D. Wright, Antibacterial drug discovery in the resistance era, Nature 529 (2016) 336–343.
[6] M. Teuber, Veterinary use and antibiotic resistance, Curr. Opin. Microbiol. 4 (2001) 493–499.
[7] T. Gottlieb, G.R. Nimmo, Antibiotic resistance is an emerging threat to public health: an urgent call to action at the Antimicrobial Resistance, Med. J. Aust. 194 (2011) 281–283.
[8] S. Pestka, Studies on the formation of transfer ribonucleic acid-ribosome complexes: viii. Survey of the effect of antibiotics on N-acetyl-phenylalanyl-puromycin formation: possible mechanism of chloramphenicol action, Arch. Biochem. Biophys. 136 (1970) 80–88.
[9] R. Sams, Florfenicol: chemistry and metabolism of a novel broad-spectrum antbiotic, Tieraerztl. Umsch. (1995).
[10] M. Cannon, S. Harford, J. Davies, A comparative study on the inhibitory actions of chloramphenicol, thiamphenicol and some fluorinated derivatives, J. Antimicrob. Chemother. 26 (1990) 307–317.
[11] H.-T. Lai, J.-H. Hou, C.-I. Su, C.-L. Chen, Effects of chloramphenicol, florfenicol, and thiamphenicol on growth of algae Chlorella pyrenoidosa, Isochrysis galbana, and Tetraselmis chui, Ecotoxicol. Environ. Saf. 72 (2009) 329–334.
[12] S.K. Yadav, B. Agrawal, P. Chandra, R.N. Goyal, In vitro chloramphenicol detection in a Haemophilus influenza model using an aptamer-polymer based electrochemical biosensor, Biosens. Bioelectron. 55 (2014) 337–342.
[13] K. Abnous, N.M. Danesh, M. Ramezani, A.S. Emrani, S.M. Taghdisi, A novel colorimetric sandwich aptasensor based on an indirect competitive enzyme-free method for ultrasensitive detection of chloramphenicol, Biosens. Bioelectron. 78 (2016) 80–86.
[14] V. Syriopoulou, A. Harding, D. Goldmann, A.L. Smith, In vitro antibacterial activity of fluorinated analogs of chloramphenicol and thiamphenicol, Antimicrob. Agents Chemother. 19 (1981) 294–297.
[15] S.J. Shin, S.G. Kang, R. Nabin, M.L. Kang, H.S. Yoo, Evaluation of the antimicrobial activity of florfenicol against bacteria isolated from bovine and porcine respiratory disease, Vet. Microbiol. 106 (2005) 73–77.
[16] S. Pilehvar, K. Gielkens, S.A. Trashin, F. Dardenne, R. Blust, K.D. Wael, (Electro) sensing of phenicol antibiotics – a review, Crit. Rev. Food Sci. Nutr. 56 (2016) 2416–2429.
[17] J.V. Samsonova, A. Cannavan, C.T. Elliott, A critical review of screening methods for the detection of chloramphenicol, thiamphenicol, and florfenicol residues in foodstuffs, Crit. Rev. Anal. Chem. 42 (2012) 50–78.
[18] J. Hayes, Determination of florfenicol in fish feeds at high inclusion rates by HPLC-UV, J. AOAC Int. 96 (2013) 7–11.
[19] Y. Yikilmaz, A. Filazi, Detection of florfenicol residues in salmon trout via GC–MS, Food Anal. Methods 8 (2015) 1027–1033.
[20] J.-E. Wu, C. Chang, W.-P. Ding, D.-P. He, Determination of florfenicol amine residues in animal edible tissues by an indirect competitive ELISA, J. Agric. Food Chem. 56 (2008) 8261–8267.
[21] F.-G. Banica, Chemical Sensors and Biosensors: Fundamentals and Applications, John Wiley & Sons, Chichester,UK, 2012.
[22] B. Van Dorst, J. Mehta, K. Bekaert, E. Rouah-Martin, W. De Coen, P. Dubruel, R. Blust, J. Robbens, Recent advances in recognition elements of food and environmental biosensors: a review, Biosens. Bioelectron. 26 (2010) 1178–1194.
[23] F. Chen, Q. Qing, J. Xia, N. Tao, Graphene field-effect transistors: electrochemical gating, interfacial capacitance, and biosensing applications, Chem. Asian J. 5 (2010) 2144–2153.
[24] A.K. Geim, K.S. Novoselov, The rise of graphene, Nat. Mater. 6 (3) (2007) 183–191.
[25] K.S. Novoselov, A.K. Geim, S.V. Morozov, D. Jiang, Y. Zhang, S.V. Dubonos, I.V. Grigorieva, A.A. Firsov, Electric field effect in atomically thin carbon films, Science 306 (2004) 666–669.
[26] H. Chang, L. Tang, Y. Wang, J. Jiang, J. Li, Graphene fluorescence resonance energy transfer aptasensor for the thrombin detection, Anal. Chem. 82 (2010) 2341–2346.
[27] H. Dong, W. Gao, F. Yan, H. Ji, H. Ju, Fluorescence resonance energy transfer between quantum dots and graphene oxide for sensing biomolecules, Anal. Chem. 82 (2010) 5511–5517.
[28] Y. Wang, Z. Li, D. Hu, C.-T. Lin, J. Li, Y. Lin, Aptamer/graphene oxide nanocomplex for in situ molecular probing in living cells, J. Am. Chem. Soc. 132 (2010) 9274–9276.
[29] Y. Wen, F. Xing, S. He, S. Song, L. Wang, Y. Long, D. Li, C. Fan, A graphene-based fluorescent nanoprobe for silver (I) ions detection by using graphene oxide and a silver-specific oligonucleotide, ChemComm 46 (2010) 2596–2598.
[30] R. Swathi, K. Sebastian, Resonance energy transfer from a dye molecule to graphene, J. Chem. Phys. 129 (2008) 054703.
[31] R. Swathi, K. Sebastian, Long range resonance energy transfer from a dye molecule to graphene has (distance) − 4 dependence, J. Chem. Phys. 130 (2009) 086101.
[32] J. Feigon, T. Dieckmann, F.W. Smith, Aptamer structures from A to ζ, Chem. Biol. 3 (1996) 611–617.
[33] C. Tuerk, L. Gold, Systematic evolution of ligands by exponential enrichment: rna ligands to bacteriophage T4 DNA polymerase, Science 249 (1990) 505–510.
[34] D. Mann, C. Reinemann, R. Stoltenburg, B. Strehlitz, In vitro selection of DNA aptamers binding ethanolamine, Biochem. Biophys. Res. Commun. 338 (2005) 1928–1934.
[35] G.J. Connell, M. Illangesekare, M. Yarus, Three small ribooligonucleotides with specific arginine sites, Biochemistry 32 (1993) 5497–5502.
[36] A.D. Ellington, J.W. Szostak, In vitro selection of RNA molecules that bind specific ligands, Nature 346 (1990) 818.
[37] Z. Tang, D. Shangguan, K. Wang, H. Shi, K. Sefah, P. Mallikratchy, H.W. Chen, Y. Li, W. Tan, Selection of aptamers for molecular recognition and characterization of cancer cells, Anal. Chem. 79 (2007) 4900–4907.
[38] B. Jin, S. Wang, M. Lin, Y. Jin, S. Zhang, X. Cui, Y. Gong, A. Li, F. Xu, T.J. Lu, Upconversion nanoparticles based FRET aptasensor for rapid and ultrasenstive bacteria detection, Biosens. Bioelectron. 90 (2017) 525–533.
[39] M. McKeague, M.C. DeRosa, Challenges and opportunities for small molecule aptamer development, J. Nucleic Acids 2012 (2012) 1–20.
[40] H. Ulrich, A.H.B. Martins, J.B. Pesquero, RNA and DNA aptamers in cytomics analysis, Cytom. Part A 59 (2004) 220–231.
[41] G. Mayer, M.-S.L. Ahmed, A. Dolf, E. Endl, P.A. Knolle, M. Famulok, Fluorescence-activated cell sorting for aptamer SELEX with cell mixtures, Nat. Protoc. 5 (2010) 1993–2004.
[42] M. Avci-Adali, A. Paul, N. Wilhelm, G. Ziemer, H.P. Wendel, Upgrading SELEX technology by using lambda exonuclease digestion for single-stranded DNA generation, Molecules 15 (2009) 1–11.
[43] M. Zuker, Mfold web server for nucleic acid folding and hybridization prediction, Nucleic Acids Res. 31 (2003) 3406–3415.

[44] M. Girardot, P. Gareil, A. Varenne, Interaction study of a lysozyme-binding aptamer with mono- and divalent cations by ACE, Electrophoresis 31 (2010) 546–555.
[45] J. Liu, Y. Lu, Preparation of aptamer-linked gold nanoparticle purple aggregates for colorimetric sensing of analytes, Nat. Protoc. 1 (2006) 246.
[46] M. Zhang, B.-C. Yin, W. Tan, B.-C. Ye, A versatile graphene-based fluorescence "on/off" switch for multiplex detection of various targets, Biosens. Bioelectron. 26 (2011) 3260–3265.
[47] M. Wu, R. Kempaiah, P.-J.J. Huang, V. Maheshwari, J. Liu, Adsorption and desorption of DNA on graphene oxide studied by fluorescently labeled oligonucleotides, Langmuir 27 (2011) 2731–2738.
[48] A. Tabasi, A. Noorbakhsh, E. Sharifi, Reduced graphene oxide-chitosan-aptamer interface as new platform for ultrasensitive detection of human epidermal growth factor receptor 2, Biosens. Bioelectron. 95 (2017) 117–123.
[49] K. Ghanbari, M. Roushani, A. Azadbakht, Ultra-sensitive aptasensor based on a GQD nanocomposite for detection of hepatitis C virus core antigen, Anal. Biochem. 534 (2017) 64–69.
[50] P. Li, Y. Qiu, H. Cai, Y. Kong, Y. Tang, D. Wang, M. Xie, Simultaneous determination of chloramphenicol, thiamphenicol, and florfenicol residues in animal tissues by gas chromatography/mass spectrometry, Chin. J. Chromatogr. 24 (2006) 14–18.
[51] P. Luo, H. Jiang, Z. Wang, C. Feng, F. He, J. Shen, Simultaneous determination of florfenicol and its metabolite florfenicol amine in swine muscle tissue by a heterologous enzyme-linked immunosorbent assay, J. AOAC Int. 92 (2009) 981–988.
[52] A.P. Pfenning, J.E. Roybal, H.S. Rupp, S.B. Turnipseed, S.A. Gonzales, J.A. Hurlbut, Simultaneous determination of residues of chloramphenicol, florfenicol, florfenicol amine, and thiamphenicol in shrimp tissue by gas chromatography with electron capture detection, J. AOAC Int. 83 (2000) 26–30.
[53] T. Nagata, H. Oka, Detection of residual chloramphenicol, florfenicol, and thiamphenicol in yellowtail fish muscles by capillary gas chromatography− mass spectrometry, J. Agric. Food Chem. 44 (1996) 1280–1284.
[54] L. Zhao, C. Ball, Determination of chloramphenicol, flofenicol, and thiamphenicol in honey using Agilent Sampliq Opt solid-phase extraction cartridges and liquid chromatography-tandem mass spectrometry, Agil. LC/MS Newsl. (2009).
[55] L. Pezza, À. Ríos, L. Nozal, L. Arce, M. Valcárcel, Determinação simultânea de resíduos de cloranfenicol, tianfenicol e florfenicol em leite bovino por cromatografia eletrocinética micelar, Quim. Nova 29 (2006) 926–931.
[56] V. Dumont, A.-C. Huet, I. Traynor, C. Elliott, P. Delahaut, A surface plasmon resonance biosensor assay for the simultaneous determination of thiamphenicol, florefenicol, florefenicol amine and chloramphenicol residues in shrimps, Anal. Chim. Acta 567 (2006) 179–183.
[57] S. Ge, M. Yan, X. Cheng, C. Zhang, J. Yu, P. Zhao, W. Gao, On-line molecular imprinted solid-phase extraction flow-injection fluorescence sensor for determination of florfenicol in animal tissues, J. Pharm. Biomed. Anal. 52 (2010) 615–619.
[58] P. Kowalski, I. Olędzka, H. Lamparczyk, Capillary electrophoresis in analysis of veterinary drugs, J. Pharm. Biomed. Anal. 32 (2003) 937–947.
[59] Y. Miao, N. Gan, T. Li, Y. Cao, F. Hu, Y. Chen, An ultrasensitive fluorescence aptasensor for chloramphenicol based on FRET between quantum dots as donor and the magnetic SiO 2@ Au NPs probe as acceptor with exonuclease-assisted target recycling, Sens Actuators B Chem. 222 (2016) 1066–1072.
[60] M. Alibolandi, F. Hadizadeh, F. Vajhedin, K. Abnous, M. Ramezani, Design and fabrication of an aptasensor for chloramphenicol based on energy transfer of CdTe quantum dots to graphene oxide sheet, Mater. Sci. Eng. C 48 (2015) 611–619.
[61] K. Paek, H. Yang, J. Lee, J. Park, B.J. Kim, Efficient colorimetric pH sensor based on responsive polymer–quantum dot integrated graphene oxide, ACS Nano 8 (2014) 2848–2856.
[62] W. Xu, Y. Lu, Label-free fluorescent aptamer sensor based on regulation of malachite green fluorescence, Anal. Chem. 82 (2009) 574–578.
[63] Y. Wang, N. Gan, Y. Zhou, T. Li, Y. Cao, Y. Chen, Novel single-stranded DNA binding protein-assisted fluorescence aptamer switch based on FRET for homogeneous detection of antibiotics, Biosens. Bioelectron. 87 (2017) 508–513.
[64] S. Wu, H. Zhang, Z. Shi, N. Duan, C. Fang, S. Dai, Z. Wang, Aptamer-based fluorescence biosensor for chloramphenicol determination using upconversion nanoparticles, Food Control. 50 (2015) 597–604.
[65] Y.-B. Miao, N. Gan, H.-X. Ren, T. Li, Y. Cao, F. Hu, Y. Chen, Switch-on fluorescence scheme for antibiotics based on a magnetic composite probe with aptamer and hemin/G-quadruplex coimmobilized nano-Pt–luminol as signal tracer, Talanta 147 (2016) 296–301.
[66] Y. Duan, L. Wang, Z. Gao, H. Wang, H. Zhang, H. Li, An aptamer-based effective method for highly sensitive detection of chloramphenicol residues in animal-sourced food using real-time fluorescent quantitative PCR, Talanta 165 (2017) 671–676.
[67] L. Zhou, N. Gan, Y. Zhou, T. Li, Y. Cao, Y. Chen, A label-free and universal platform for antibiotics detection based on microchip electrophoresis using aptamer probes, Talanta 167 (2017) 544–549.
[68] S. Pilehvar, J. Mehta, F. Dardenne, J. Robbens, R. Blust, K. De Wael, Aptasensing of chloramphenicol in the presence of its analogues: reaching the maximum residue limit, Anal. Chem. 84 (2012) 6753–6758.
[69] S. Pilehvar, F. Dardenne, R. Blust, K. De Wael, Electrochemical sensing of phenicol antibiotics at gold, Int. J. Electrochem. Sci. 7 (2012) 5000–5011.
[70] S. Bamrungsap, M.I. Shukoor, T. Chen, K. Sefah, W. Tan, Detection of lysozyme magnetic relaxation switches based on aptamer-functionalized superparamagnetic nanoparticles, Anal. Chem. 83 (2011) 7795–7799.
[71] Y.F. Duan, Y. Ning, Y. Song, L. Deng, Fluorescent aptasensor for the determination of Salmonella typhimurium based on a graphene oxide platform, Mikrochim. Acta 181 (2014) 647–653.